

GT2011-46385

## IDENTIFYING TURBULENT SPOTS IN TRANSITIONAL BOUNDARY LAYERS

**Brendan Rehill \***

**Ed J. Walsh**

Stokes Institute  
University of Limerick  
Limerick  
Ireland

Email: brendan.rehill@ul.ie

**Philipp Schlatter**

**Luca Brandt**

Linné Flow Centre  
KTH Mechanics  
Stockholm  
Sweden

**Tamer A. Zaki**

Department of Mechanical Engineering  
Imperial College London  
London  
UK

**Donald M. McEligot**

Mechanical Engineering Department  
University of Idaho  
Idaho Falls, Idaho, 83402

### ABSTRACT

*An artificial turbulent spot is simulated in a zero free-stream turbulence base flow and a base flow with organised streaks. Six identification methods are used in order to isolate the turbulent spot from the surrounding non-turbulent fluid. These are (i) instantaneous wall-normal velocity,  $v'$ , (ii) instantaneous spanwise velocity,  $w'$ , (iii) instantaneous turbulent dissipation, (iv)  $\lambda_2$  - criterion, (v)  $Q$  - criterion and (vi) gradient of the Finite Time Lyapunov Exponent. All methods are effective in isolating the turbulent spot from the streaks. The robustness of each technique is determined from the sensitivity of the maximum spot dimensions to changes in threshold level. The  $Q$  - criterion shows the least sensitivity for the zero free-stream turbulence case and the instantaneous turbulent dissipation technique is least sensitive in the organised streaks case. For both cases the  $v'$  technique was the most sensitive to changes in threshold level.*

### NOMENCLATURE

$FST$  free-stream turbulence  
 $Re$  Reynolds number  
 $u$  instantaneous streamwise velocity  
 $U_\infty$  free-stream velocity  
 $v$  instantaneous wall-normal velocity  
 $v'$  instantaneous wall-normal fluctuating velocity  
 $w$  instantaneous spanwise velocity  
 $w'$  instantaneous spanwise fluctuating velocity  
 $x$  streamwise coordinate  
 $y$  wall-normal coordinate  
 $z$  spanwise coordinate  
 $\delta_0^*$  displacement thickness at beginning of computational domain  
 $\nu$  dynamic viscosity

---

\*brendan.rehill@ul.ie

## INTRODUCTION

The transition region in boundary layers is important in many engineering applications. In particular, in gas turbine engines, transition-to-turbulence can occupy up to 70% of the axial chord in the low-pressure stages of the turbine [1] and can be promoted by the adverse pressure gradient condition in the compressor stages [2, 3]. The transitional boundary layer consists of juxtaposed zones of turbulent and non-turbulent flow. Emmons [4] was the first to identify these localised patches of turbulence, termed turbulent spots. They were observed to appear irregularly in time and space with significantly different flow properties than the surrounding non-turbulent fluid [4]. Thus, turbulent spots were established as an essential feature in the transition to turbulent flow. Understanding the evolution of these spots is key to increasing the efficiency of such systems in terms of heat, mass and momentum transport and may have important implications for the development of improved transition models to predict heat transfer and losses for turbine blades.

There are two distinct paths to boundary layer transition, and both involve the appearance of turbulent spots. The first is natural, or classical, transition and is observed when the free-stream turbulence intensity is very low. Disturbances appear in the laminar boundary layer in the form of two-dimensional Tollmien-Schlichting waves. Downstream, the instability develops into three-dimensional waves and vortices emerge. In regions of high local vorticity, bursts of turbulence occur in the form of turbulent spots [5]. The second type is termed bypass transition and occurs where there is free-stream turbulence greater than approximately 1%, the case of interest in examining transition in gas turbines. Jacobs & Durbin [6] identified some important aspects of bypass transition such as the laminar boundary layer buffeted by free-stream turbulence. Low-frequency modes from the free-stream turbulence penetrate the boundary layer [7] leading to elongated streaks of high and low-speed fluid [8]. These streaks then break down into turbulent spots characterised by a region of intermittent spot formation. The spots grow and eventually coalesce to form the fully turbulent boundary layer.

Schubauer & Klebanoff [9] were the first to describe the growth characteristics of turbulent spots such as leading and trailing edge velocities, which scaled with free-stream velocity, and the typical arrowhead shape of these spots. They used hot-wire anemometry to analyse an artificial turbulent spot in an otherwise laminar boundary layer. Identifying the spot was done by examining the rapid change in the hot-wire signal at the leading edge of the spot. Gad-el-hak & Riley [10] established some general characteristics of turbulent spots in laminar boundary layers, such as the leading edge turbulent region overhanging non-turbulent fluid closer to the wall. Sankaran et al. [11] differentiated and squared the hot-wire signal in order to emphasize the high frequency components. Singer [12] examined an artificial turbulent spot generated by an injection of air through a blowing slot. The leading and trailing edges of the turbulent spot were de-

finied along the centreline as the furthest point downstream and upstream where  $|\partial u/\partial x| \geq 0.02$ . The spanwise extent of the spot is defined as the maximum  $z$  location, for all  $x$  and  $y$ , where  $|\partial u/\partial x| \geq 0.02$ . Ching & LaGraff used the heat flux at the wall to identify naturally occurring turbulent spots [13]. Jocksch & Kleiser [14] used the spanwise vorticity in examining the shape of the turbulent spot, setting a threshold of  $|\omega_z| = 0.1$ .

In recent years, much work has focused on trying to identify coherent structures in both fully developed turbulence and transitional flows. Some of these techniques can be used to identify a turbulent spot which is a collection of coherent structures. Green et al. [15] compared some Eulerian techniques to the Lagrangian technique of using Direct Lyapunov Exponents (DLE) to identify coherent structures in a single isolated hairpin vortex and a fully developed turbulent flow. While the DLE was computationally more expensive, it did provide several advantages such as greater detail in that the DLE can be evaluated on a finer grid than the original velocity field. They also noted that the outer shape of the structures did not change with increased integration time, just the detail of the structure.

Volino et al. [16] performed experiments on turbulent spots generated with free-stream turbulence of 8% which showed that there were significant differences in the mean velocity profiles between the turbulent and non-turbulent zones in the transition region. Volino et al. [16] also showed significantly higher wall-normal fluctuations and turbulent shear stress in the turbulent spot with the skin friction being as much as 70% higher within the spot than in the non-turbulent zone. Mean velocities within artificial turbulent spots were found to significantly differ from both the surrounding non-turbulent flow and fully turbulent profiles [17]. These observations that the turbulent spots show significant differences from non-turbulent flow and fully turbulent flow highlight the limitations of traditional transition models which assume either laminar or fully turbulent states, or fail to treat the turbulent and non-turbulent parts separately. It also highlights the importance of a robust technique to avoid contamination of the spot from the non-turbulent flow. Statistics and other quantities from the isolated turbulent spot may give insight into how turbulence develops and sustains itself. To obtain these statistics, the turbulent spot must be treated independently from the surrounding non-turbulent flow and this approach is known as conditional sampling. Many techniques have been used to conditionally sample the flow including derivatives of the instantaneous streamwise velocity fluctuations,  $u'$ , or instantaneous turbulent shear stress,  $-u'v'$  [16]. With many different identification techniques come variations in spot properties. While Schubauer & Klebanoff [9] observed trailing edge convection speed of  $0.5U_e$ , Gutmark & Blackwelder [18] reported  $0.58U_e$ , and Singer [12] reported  $0.63U_e$ . This variation could be attributed to the difference in identification techniques and motivates the need for a robust identification technique.

The ultimate goal is to examine naturally occurring spots in

a transitional boundary layer subject to free-stream turbulence. The current work aims to examine artificial turbulent spots and to assess the robustness of the methods used for detecting them. Direct numerical simulations of a single turbulent spot, artificially generated by a vortex pair, are studied under two different free-stream conditions; 1) a zero free-stream turbulence Blasius base flow and 2) a base flow of organised streaks. Similiar vortex pair disturbances have previously been used to trigger turbulent spots in direct numerical simulations [14, 19]. Six different methods of spot identification are employed where thresholds are set for: (i) instantaneous wall-normal velocity,  $v'$ , (ii) instantaneous spanwise velocity,  $w'$ , (iii) instantaneous turbulent dissipation, (iv)  $\lambda_2$  - criterion, (v)  $Q$  - criterion and (vi) Finite Time Lyapunov Exponent (FTLE) gradient. The sensitivity of the spot dimensions to changes in threshold level is used to assess the robustness of the identification techniques. The need for filtering and smoothing post application of threshold level is also to be taken into account.

## NUMERICAL METHOD

A zero-pressure gradient laminar boundary layer flow with artificially triggered turbulent spots is examined. Direct numerical simulations of a flat plate boundary layer were performed using a code developed at KTH Mechanics [20]. The three-dimensional, time-dependent, incompressible Navier-Stokes equations are solved using spectral methods. The computational domain is periodic in the streamwise and spanwise directions, and is discretised using Fourier series. In the wall-normal direction Chebyshev polynomials are used. Time integration is performed using a third order Runge-Kutta method for the advective and forcing terms and a Crank-Nicolson method for the viscous terms. The inflow is at Reynolds number  $Re_{\delta_0^*} = U_\infty \delta_0^* / \nu = 300$ , where  $\delta_0^*$  is the displacement thickness at the beginning of the computational domain,  $U_\infty$  is the free-stream velocity and  $\nu$  is the fluid viscosity. All velocities and lengths are nondimensionalised with respect to  $U_\infty$  and  $\delta_0^*$ . The coordinates  $x$ ,  $y$  and  $z$  refer, respectively to the streamwise, wall-normal and spanwise directions, with  $u$ ,  $v$  and  $w$  the corresponding velocity components. A fringe region is employed in the streamwise direction where the flow is smoothly forced to the desired inflow velocity. Two different prescribed velocity fields will be examined in this paper, namely Blasius base flow with zero free-stream turbulence and a base flow of organised steady streaks. In addition, a vortex pair disturbance is added to the velocity field at a streamwise position of  $x = 60\delta_0^*$ . This disturbance breaks down into an artificial turbulent spot. The dimensions of the computational domain are  $700\delta_0^*$ ,  $30\delta_0^*$  and  $300\delta_0^*$  in the  $x$ ,  $y$  and  $z$  directions respectively, with corresponding resolutions of 768, 121 and 384. Streamwise velocity in an  $x$ - $z$  plane at a wall-normal position of  $y/\delta_0^* = 4$  is shown in Fig. 1 for each flow scenario. The first is a single turbulent spot in a Blasius base flow with zero free-stream

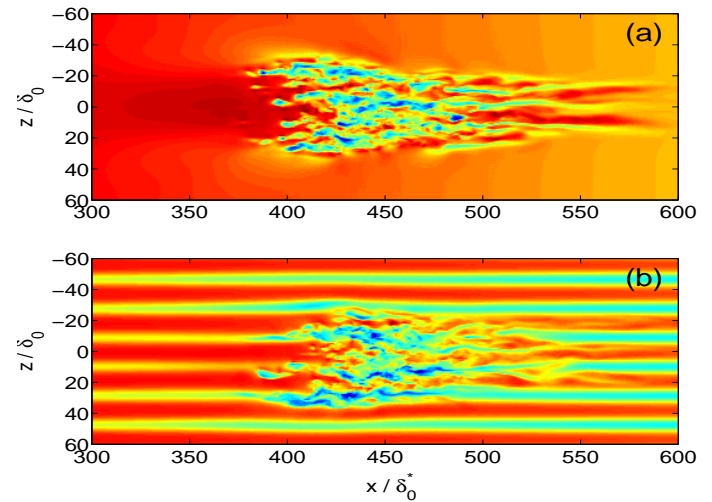


**FIGURE 1.** STREAMWISE VELOCITY IN AN X-Z PLANE AT A WALL-NORMAL POSITION OF  $y/\delta_0^* = 4$ . (a) ZERO FREE-STREAM TURBULENCE (b) ORGANISED STREAKS

turbulence, Fig. 1 (a). The second is a single turbulent spot in the presence of organised streaks which have been forced in the fringe region, Fig. 1 (b). For all flow cases the spot is artificial in that it is generated by the vortex pair disturbance. The amplitude of the organised streaks was chosen at a level to ensure turbulent spot formation through streak breakdown did not occur within the domain.

## IDENTIFICATION TECHNIQUES

The methods of identification employed in the current study are setting threshold levels for:

- (i) instantaneous wall-normal velocity,  $v'$
- (ii) instantaneous spanwise velocity,  $w'$
- (iii) instantaneous turbulent dissipation
- (iv)  $\lambda_2$  - criterion
- (v)  $Q$  - criterion
- (vi) Finite Time Lyapunov Exponent gradient. (FTLE)

Techniques (i) - (v) are derived from the instantaneous velocity field and its gradient and are considered Eulerian while technique (vi) is a Lagrangian method. It is known that there are significant streamwise velocity fluctuations in regions outside of the turbulent spot due to the organised streaks and also due to free-stream turbulence. Streak amplitudes of over 30% of the mean flow have been reported in laminar boundary layers [21, 22]. While the streamwise velocity may be most suitable for identifying a turbulent spot in a zero free-stream turbulence case, it was deemed unsuitable as an identification technique

once additional disturbances were introduced. Instantaneous turbulent dissipation is calculated based on the dissipation function described by the equation [5]

$$\begin{aligned} \phi = & 2 \left[ \left( \frac{\partial u}{\partial x} \right)^2 + \left( \frac{\partial v}{\partial y} \right)^2 + \left( \frac{\partial w}{\partial z} \right)^2 \right] + \\ & + \left[ \left( \frac{\partial u}{\partial y} + \frac{\partial v}{\partial x} \right)^2 + \left( \frac{\partial u}{\partial z} + \frac{\partial w}{\partial x} \right)^2 + \left( \frac{\partial v}{\partial z} + \frac{\partial w}{\partial y} \right)^2 \right]. \end{aligned} \quad (1)$$

The streamwise terms of the above equation are eliminated to yield Eqn.2 which is used to calculate the instantaneous turbulent dissipation in the current study where the reference threshold is set at 1% maximum value.

$$\begin{aligned} \phi = & 2 \left[ \left( \frac{\partial v}{\partial y} \right)^2 + \left( \frac{\partial w}{\partial z} \right)^2 \right] \dots \\ & + \left[ \left( \frac{\partial v}{\partial x} \right)^2 + \left( \frac{\partial w}{\partial x} \right)^2 + \left( \frac{\partial v}{\partial z} + \frac{\partial w}{\partial y} \right)^2 \right] \end{aligned} \quad (2)$$

The Q-criterion locates regions where rotation dominates strain [23] and is based on the velocity gradient tensor,  $\nabla V$ . The velocity gradient tensor is divided into symmetric,  $S$ , and anti-symmetric parts,  $\Omega$ , given in Eqn. 3.

$$S = \frac{1}{2} [\nabla V + (\nabla V)^T] \quad \Omega = \frac{1}{2} [\nabla V - (\nabla V)^T] \quad (3)$$

The Q-criterion is given by  $Q = \frac{1}{2} (\|\Omega\|^2 - \|S\|^2)$ , where  $\|\cdot\|$  is the Euclidean matrix norm. The reference threshold for the Q-criterion was set at 1% maximum value. The  $\lambda_2$ -criterion identifies vortex cores as pressure minima in a 2-D plane perpendicular to the vortex core [24]. It is defined as the second largest eigenvalue of  $S^2 + \Omega^2$ . The reference threshold for the  $\lambda_2$ -criterion was set at 1% of its maximum value. The Finite Time Lyapunov Exponent (FTLE) provides a measure of the rate of separation of neighbouring particle trajectories [15, 25]. Unlike the other methods this is a Lagrangian technique in that particle trajectories must be calculated.

Threshold levels for techniques (i) and (ii) must be varied in the wall-normal direction and were based on streamwise- and spanwise-averaged velocity fluctuations. These thresholds need to be low near the wall in order to capture the spot signature in this area. The thresholds for techniques (i) and (ii) are shown in Fig. 2. The averaged velocity fluctuations have a peak at approximately  $y = 5\delta_0^*$  and  $y = 3\delta_0^*$  for the wall-normal and spanwise velocity respectively. Once this peak is reached the threshold is set at this level for the remaining wall-normal positions.

There are four main steps to the identification process outlined in Fig. 3 using criterion (i) as an example. The instantaneous wall-normal velocity in an x-z plane at a wall-normal position of  $y = 4\delta_0^*$  is shown in Fig. 3 (a). Figure 3 (b) shows

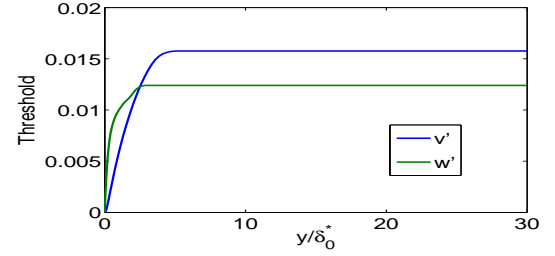


**FIGURE 2.** THRESHOLD LEVELS BASED ON STREAMWISE- AND SPANWISE-AVERAGED VELOCITY FLUCTUATIONS

the turbulent spot identified by the threshold where black represents values above the selected threshold. This representation of the spot includes white regions or holes within the turbulent spot which need to be removed in order to determine the edge of the spot. Filtering and smoothing are used to remove these holes within the turbulent spot which results in Fig. 3 (c) showing a clearly defined turbulent spot surrounded by non-turbulent flow. For each cell of the computational domain, the filtering process determines how many of the neighbouring cells are turbulent and how many are non-turbulent. If more turbulent cells than non-turbulent cells are in the vicinity then the original cell is switched to turbulent. The edge of the identified turbulent spot is then superimposed on to the original instantaneous spanwise velocity plot as shown in Fig. 3 (d) where the black line indicates the edge of the turbulent spot. The same procedure is used for all techniques with filtering required for all identification methods used in this study. The Lagrangian FTLE method alone fails to elucidate the turbulent spot from the surrounding streaks. It was not possible to set a sensible threshold that would eliminate the streaks while retaining the features of the turbulent spot. The problem with the FTLE method is highlighted in Fig. 4 (a) in that streaks are detected. Due to the presence of streaks in the flow the particles on the boundary of the high and low-speed streaks will have significantly different trajectories, hence the FTLE field will highlight this as seen in Fig. 4 (a). This would suggest that it is a poor method for identifying natural turbulent spots in a transitional flow as the technique cannot isolate the spot region from the surrounding streaks. However, the gradient of this method, Fig. 4 (b), which clearly isolates the spot from the surrounding streaks, could be used.

## RESULTS AND DISCUSSION

The identification techniques were applied to a single turbulent spot with zero free-stream turbulence and zero pressure gradient base flow. Visualisations of the spot shape at a wall-parallel plane,  $y/\delta_0^* = 4$ , are shown in Fig. 5, with the spot edge denoted by the solid black line. Differences can be seen in the spot shape depending on identification technique used. The  $w'$

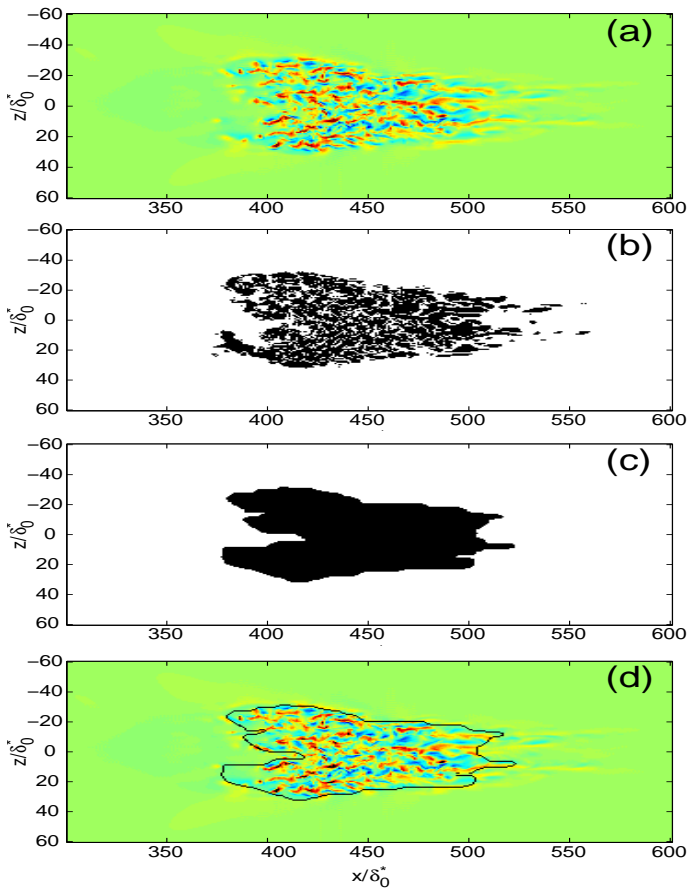


**FIGURE 3.** VISUALISATION OF WALL-PARALLEL PLANE AT  $y/\delta_0^*=4$  SHOWING TYPICAL IDENTIFICATION PROCEDURE. (a) INSTANTANEOUS WALL-NORMAL VELOCITY, (b) THRESHOLD APPLIED, BLACK DENOTES REGIONS ABOVE THIS THRESHOLD (c) FILTERING AND SMOOTHING TO REMOVE HOLES WITHIN THE SPOT (d) EDGE OF TURBULENT SPOT DENOTED BY BLACK LINE SUPERIMPOSED ON ORIGINAL WALL-NORMAL VELOCITY IMAGE

and FTLE gradient method identify the spot extending further in the streamwise direction than the other methods. This indicates high levels of spanwise velocity at the leading edge. Also, the FTLE method is heavily influenced by the streamwise velocity component. As can be seen in Fig. 1 two high streamwise velocity regions appear at the leading edge of the spot. Singer [12] observed similarly strong streamwise velocity just off the centreline in his DNS data of an artificial spot. Seifert et al. [26] also identified the leading edge flow being dominated by significant streamwise and spanwise fluctuations in their experiments on an artificial turbulent spot in a laminar boundary layer. The spot identified by the dissipation technique does not include this area of the flow. This can be explained by the elimination of the

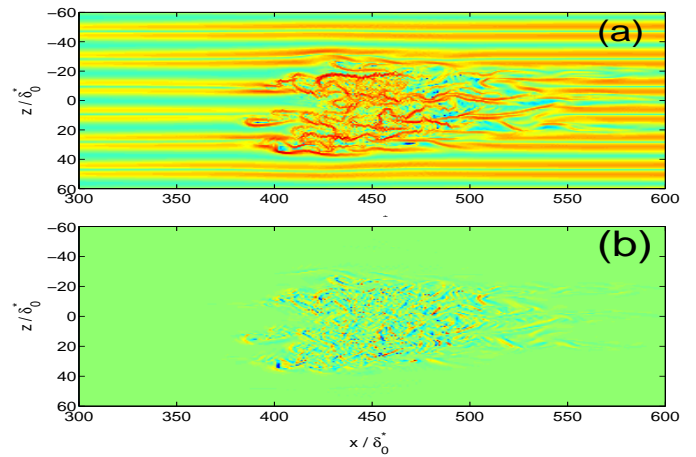


**FIGURE 4.** VORTEX PAIR + ORGANISED STREAKS: (a) XZ PLANE OF FTLE FIELD AT WALL-PARALLEL PLANE AT  $y/\delta_0^*=4$ , (b) STREAMWISE GRADIENT OF FTLE FIELD AT THE SAME WALL-PARALLEL PLANE. THIS ISOLATES THE SPOT FROM THE SURROUNDING STREAKS.

streamwise components from the dissipation equation (Eqn. 2). The high streamwise velocity region or calmed region, a characteristic of these artificial turbulent spots [10], can be seen at the trailing edge of the spot in Fig. 1. Low-velocity streaks from the turbulent spot extend into the calmed region similar to spots observed by Schröder & Kompenhans [27]. Two low-velocity streaks can be observed at the wingtips which are well identified by the  $\lambda_2$  and  $Q$  – criterion in Fig. 5. These wingtips are also similar to the artificial spot identified by Singer [12]. Schröder & Kompenhans [27] suggest that these streaks from the turbulent spot extending into the calmed region may be the principal mechanism for turbulence generation and therefore an identification method which clearly identifies them would be of critical importance, thereby placing  $\lambda_2$  and  $Q$  as good techniques for capturing important aspects of the turbulent spot.

The identification techniques were then applied to the single turbulent spot in the presence of organised streaks. Again the shapes vary depending on which technique is used. The effect of the streaks is pronounced at both the leading and trailing edges of the spot as seen from the streamwise velocity components in Fig. 1. At the leading edge of the spot where there were two distinct high streamwise velocity regions either side of the centreline, there is now a high velocity streak at the centreline with low velocity streaks to either side. The effect of this is highlighted in the FTLE gradient method and also indicated less obviously by the  $v'$ ,  $w'$ ,  $\lambda_2$  and  $Q$  methods shown in Fig. 6. The streak interaction with the rear of the spot is also clearly visible showing a lack of a clear calmed region in Fig. 1. The region is distorted by the low-speed organised streaks and low-speed streaks from

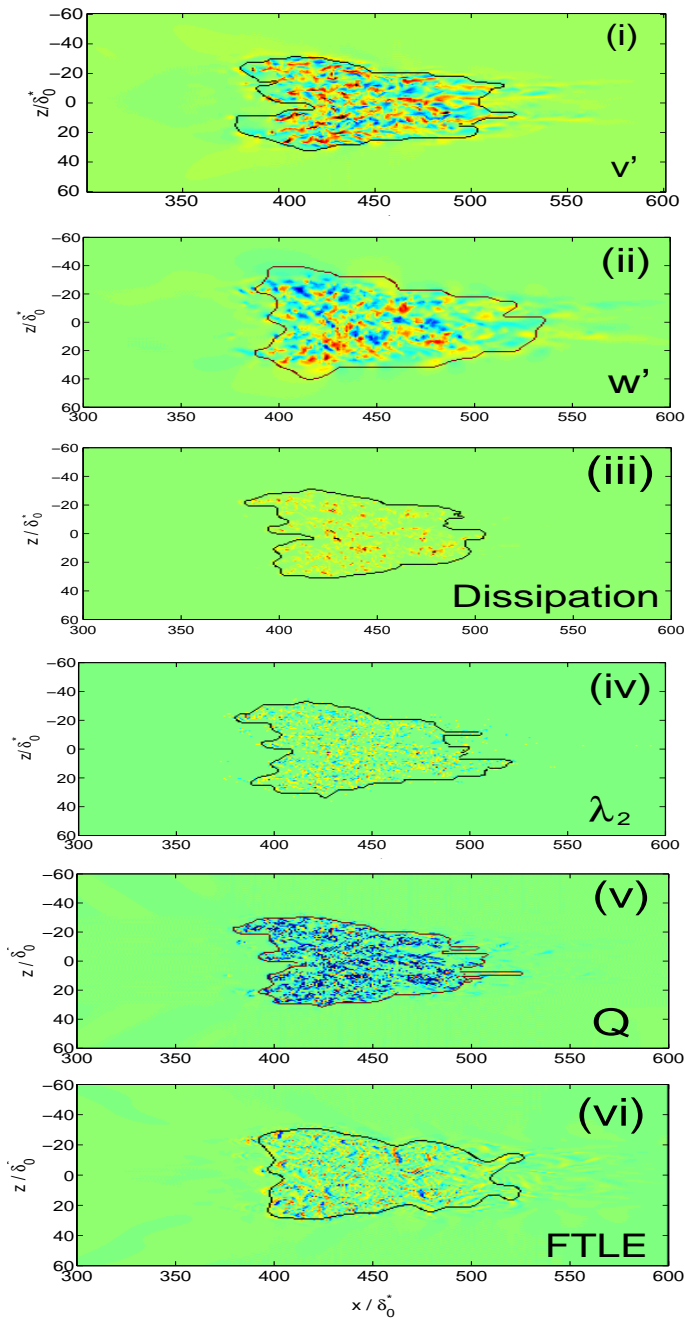


**FIGURE 5.** VORTEX PAIR + ZERO FST: VISUALISATION OF WALL-PARALLEL PLANE AT  $y/\delta_0^*=4$  SHOWING EDGE OF TURBULENT SPOT DENOTED BY THE BLACK LINE FOR EACH IDENTIFICATION METHOD. (i)  $v'$ , (ii)  $w'$ , (iii) TURBULENT DISSIPATION, (iv)  $\lambda_2$ -CRITERION, (v) Q-CRITERION AND (vi) FTLE GRADIENT. FLOW DIRECTION IS FROM LEFT TO RIGHT.

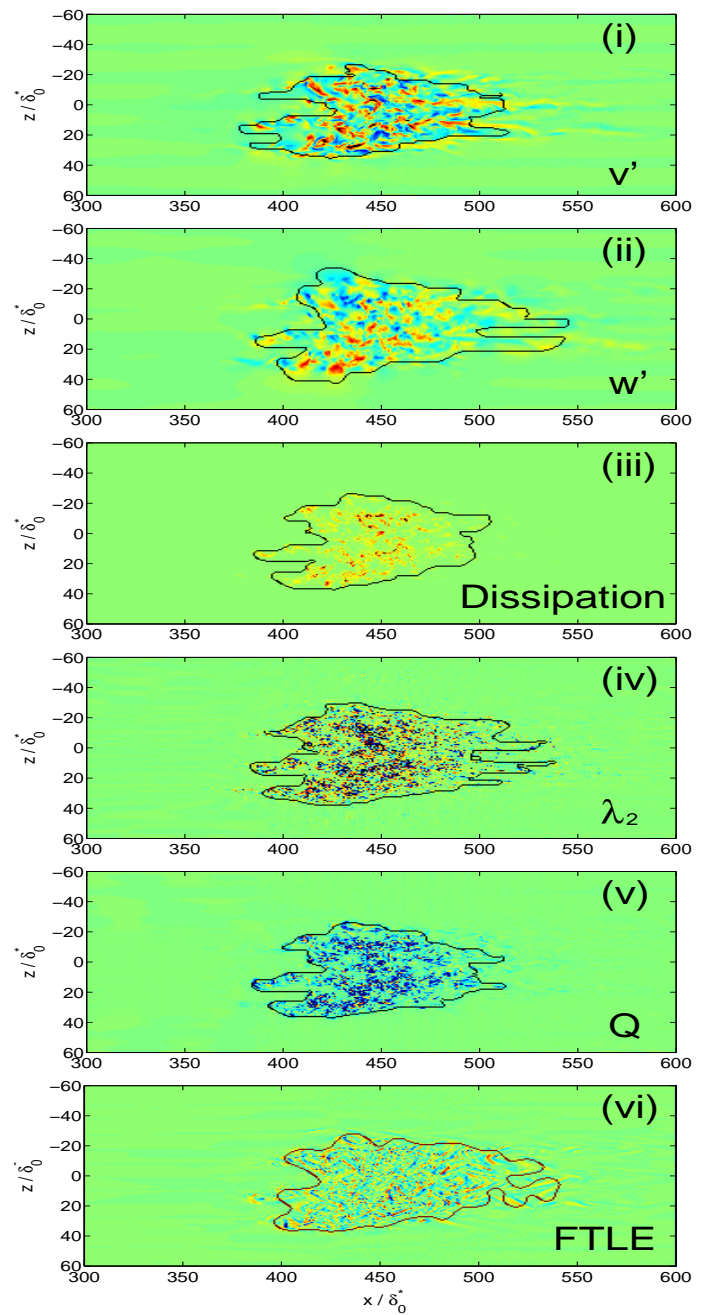


**FIGURE 6.** VORTEX PAIR + ORGANISED STREAKS: VISUALISATION OF WALL-PARALLEL PLANE AT  $y/\delta_0^*=4$  SHOWING EDGE OF TURBULENT SPOT DENOTED BY THE BLACK LINE FOR EACH IDENTIFICATION METHOD. (i)  $v'$ , (ii)  $w'$ , (iii) TURBULENT DISSIPATION, (iv)  $\lambda_2$ -CRITERION, (v) Q-CRITERION AND (vi) FTLE GRADIENT. FLOW DIRECTION IS FROM LEFT TO RIGHT.

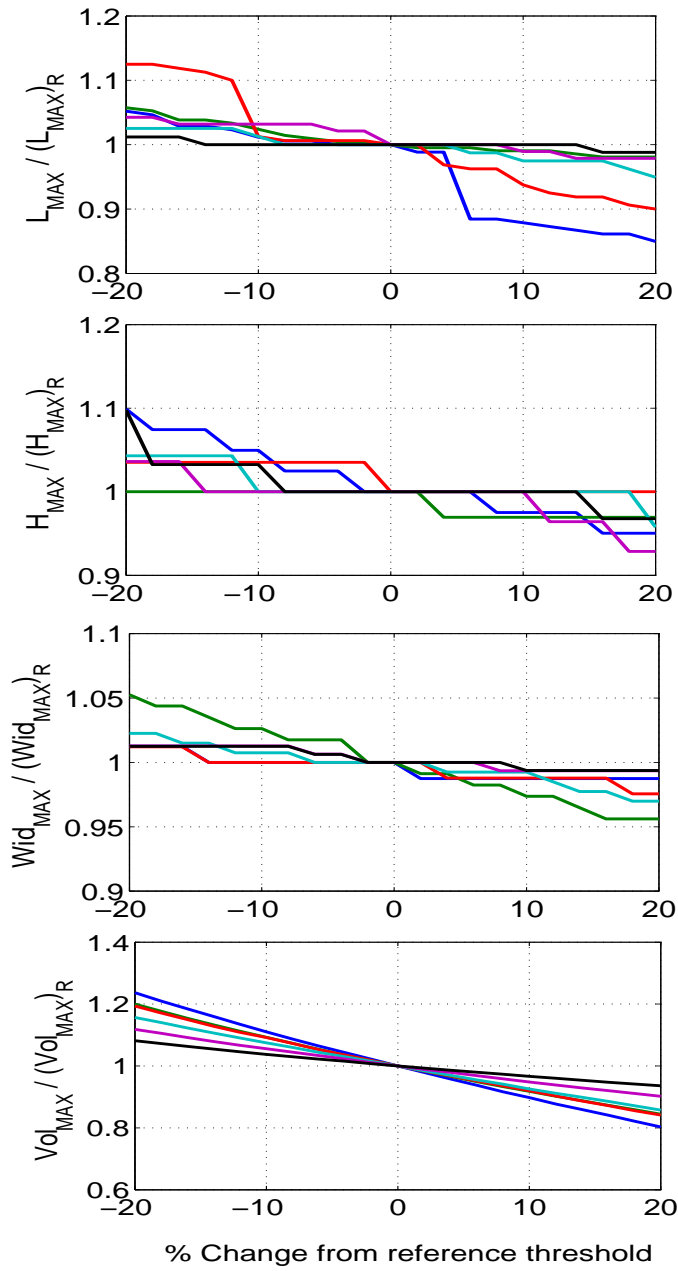


**FIGURE 7.** VORTEX PAIR + ZERO FST: SENSITIVITY ANALYSIS OF MAXIMUM SPOT DIMENSIONS TO  $\pm 20\%$  CHANGES IN THRESHOLD LEVEL. ALL DIMENSIONS ARE NORMALISED WITH RESPECT TO THE DIMENSION AT THE REFERENCE THRESHOLD VALUE (L=LENGTH, H=HEIGHT, WID=WIDTH, VOL=VOLUME). —  $v'$ , —  $w'$ , — Dissipation, —  $\lambda_2$ , —  $Q$ , — FTLE gradient

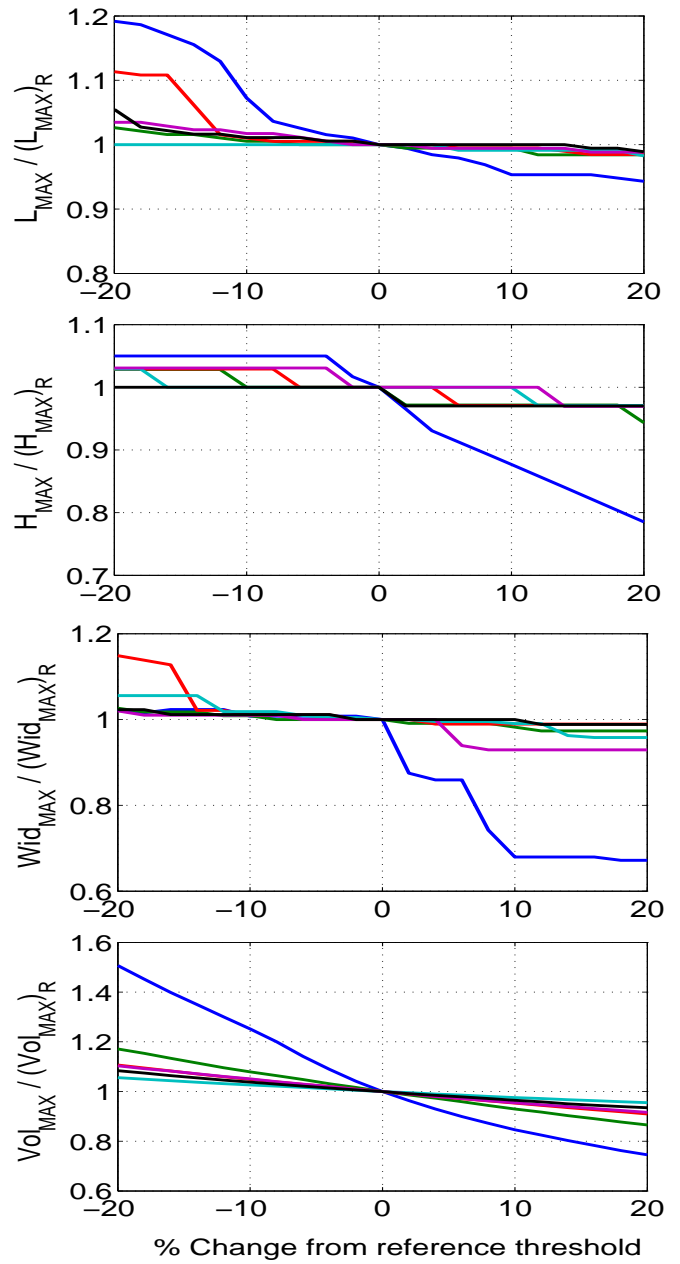


**FIGURE 8.** VORTEX PAIR + ORGANISED STREAKS: SENSITIVITY ANALYSIS OF MAXIMUM SPOT DIMENSIONS TO  $\pm 20\%$  CHANGES IN THRESHOLD LEVEL. ALL DIMENSIONS ARE NORMALISED WITH RESPECT TO THE DIMENSION AT THE REFERENCE THRESHOLD VALUE (L=LENGTH, H=HEIGHT, WID=WIDTH, VOL=VOLUME). —  $v'$ , —  $w'$ , — Dissipation, —  $\lambda_2$ , —  $Q$ , — FTLE gradient

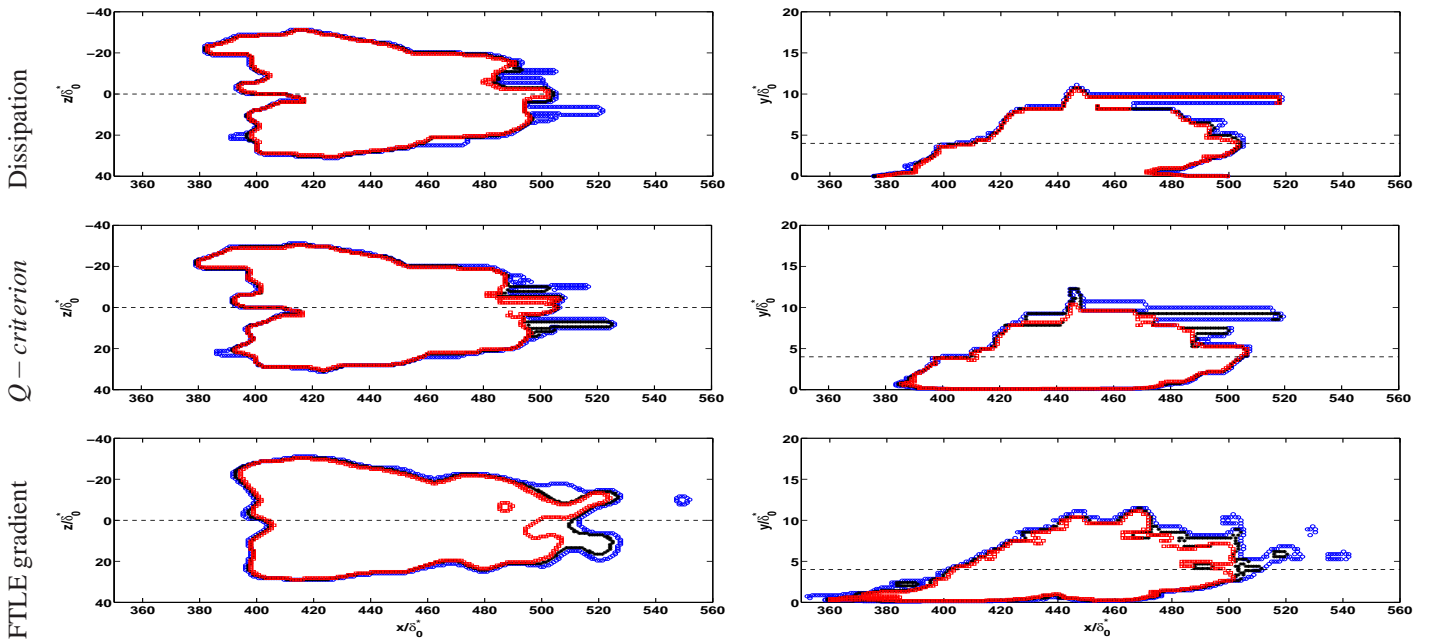


**FIGURE 9.** VORTEX PAIR + ZERO FST: CHANGE IN SPOT SHAPE WITH CHANGE IN THRESHOLD. LEFT: WALL-PARALLEL PLANE ( $y/\delta_0^*=4$ ). RIGHT: CENTRELINE WALL-NORMAL PLANE ( $z/\delta_0^*=0$ ). \* REFERENCE THRESHOLD,  $\circ$  -20% REFERENCE THRESHOLD,  $\square$  +20% REFERENCE THRESHOLD

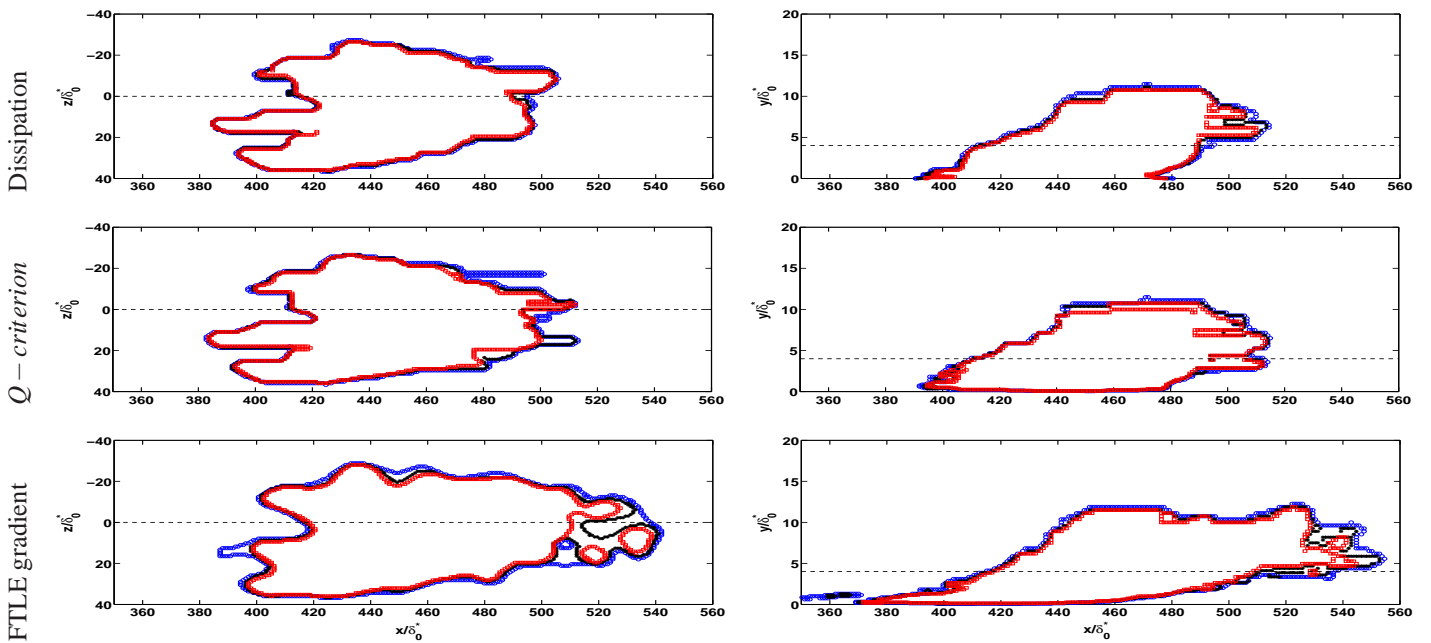


**FIGURE 10.** VORTEX PAIR + ORGANISED STREAKS: CHANGE IN SPOT SHAPE WITH CHANGE IN THRESHOLD. LEFT: WALL-PARALLEL PLANE ( $y/\delta_0^*=4$ ). RIGHT: CENTRELINE WALL-NORMAL PLANE ( $z/\delta_0^*=0$ ). \* REFERENCE THRESHOLD,  $\circ$  -20% REFERENCE THRESHOLD,  $\square$  +20% REFERENCE THRESHOLD

within the turbulent spot. All identification methods show a reduced spot length at the location of the low-speed streak while an elongation in the spot at the high-speed streak. This is observed at the outer wingtips of the spot. The wing tip identified in the zero free-stream turbulence case at  $z/\delta_0^* \approx -20$  in Fig. 5 shows a dramatic reduction in length due to the presence of the low-speed streak as shown by the identification methods in Fig. 6. The different shape characteristics in artificial and naturally-occurring turbulent spots under high free-stream turbulence conditions as studied experimentally by Matsubara & Alfredson [28] and computationally by Brandt et al. [17, 20] could be explained by the streak interactions with the turbulent spot, elongating certain regions of the spot while reducing it in others. The identification methods used can indicate the flow characteristics within the turbulent spot. It appears that dissipation is concentrated to the rear and centre of the spot. Volino et al. [16] observed near zero dissipation in non-turbulent zones which is also seen in the current study with dissipation focused in the spot for both a zero pressure gradient case and the organised streak case. Hence, if the objective is to examine turbulent statistics then this method may prove the best, since otherwise the analysis would result in averaging regions where turbulence is small.

## SENSITIVITY ANALYSIS

In order to determine the most suitable identification technique, the robustness of each is examined using a sensitivity analysis. The analysis was based on the changes in the maximum dimensions of the spot with change in threshold level. The threshold level was varied  $\pm 20\%$  around the reference threshold and the maximum width, length, height and volume of the spot were recorded to determine which was least sensitive to changes in threshold. Figure 7 shows the change in maximum spot dimensions with variation in threshold level for the single turbulent spot with zero free-stream turbulence where  $L$ ,  $H$ ,  $Wid$  and  $Vol$  refer to length, height, width and volume of the spot, respectively. These are normalised by the spot dimensions at the reference threshold denoted by the subscript  $R$ . The maximum volume of the spot gives an indication of the average change in spot dimensions with change in threshold level and therefore would reflect the overall robustness of each method. Looking at the maximum volume, the most sensitive to changes in threshold level is the  $v'$  method. The least sensitive is the  $Q$ -criterion which shows a 14% change in maximum spot volume for a  $\pm 20\%$  change in threshold level compared with a 43% change for the  $v'$  method for the same change in threshold.

Figure 8 shows the results of the sensitivity analysis performed on the single turbulent spot in the presence of organised streaks. The most sensitive to changes in threshold level in this case is again the  $v'$  method. The least sensitive for the organised streaks case is the dissipation technique with a 10% change in maximum volume of the spot for a  $\pm 20\%$  change in threshold

level. The  $Q$ -criterion also works well for this case with a 15% change in maximum spot volume. While giving a good idea of how robust the techniques are, the sensitivity analysis can also give an insight into the aspects of the flow around the spot. As a lower threshold value will include more of the flow and therefore a larger spot, while the higher thresholds would naturally exclude more of the flow. The difference then between the minimum and maximum thresholds can be thought of as the outer regions of the spot, a portion of the flow outside and a portion of the flow within the spot is captured using this analysis.

Figures 9 and 10 give more insight into the nature of the spot change with changing threshold. Spot shapes at a wall-parallel plane,  $y/\delta_0^* = 4$ , and a wall-normal plane,  $z/\delta_0^* = 0$ , are shown for the dissipation,  $Q$ -criterion and FTLE gradient techniques. The spot edges for the reference threshold and  $\pm 20\%$  threshold are overlaid on top of each other. The rear and sides of the spot show very little variation with changing threshold level. Most of the changes to the spot shape occur at the leading edge of the spot. Denton et al. [29] reported elevated dissipation levels focused near the wall. This is observed in the current study with the dissipation in the wall-normal plane (Fig. 9) showing a significant increase in the spot length close to wall. An overhang region can be seen at the front of the spot in the wall-normal plane, a typical turbulent spot characteristic [10]. Figure 9 indicates why the FTLE gradient method performed so poorly in the sensitivity analysis based on length in Fig. 7. Both the wall-parallel and wall-normal planes show significant changes in the leading edge of the spot with changes in threshold level. In the presence of streaks (Fig. 10) both the  $Q$ -criterion and dissipation techniques show only slight changes in shape with changing threshold. With the FTLE gradient method, regions of the flow at the leading edge of the spot become isolated as the threshold is increased. The streaks seem to increase the amount of turbulent flow in the overhang region which can be seen especially in the FTLE gradient method with a significant increase in the spot length at the front of the spot away from the wall. The lengthening of the spot front is also shown to a lesser extent with the dissipation and  $Q$ -criterion. Overall both the dissipation and  $Q$ -criterion show only slight variations in spot shape due to threshold variations with most changes occurring close to the leading edge of the spot.

## CONCLUSIONS

Direct numerical simulations of turbulent spots in two base flows were examined in order to determine the most suitable way to identify and isolate them from the surrounding fluid flow. Six identification methods were used and yielded differences in spot shapes. A sensitivity analysis of maximum spot dimensions with changes in threshold level indicated that the  $Q$ -criterion and dissipation methods work well in identifying the turbulent spot. They show the least sensitivity to changes in reference threshold.

These techniques work well in the presence of streaks. The most sensitive to changes in threshold level was the  $v'$  method in both cases. The effect of streaks on the shape of an artificial turbulent spot was examined with low- and high-speed streaks elongating and reducing the spot, respectively.

## ACKNOWLEDGMENT

This work has been supported by the Irish Research Council for Science, Engineering and Technology Embark Initiative.

## REFERENCES

- [1] Walsh, E. J., and Davies, M. R. D., 2004. "Measurements in the transition region of a turbine blade profile under compressible conditions". *ASME J.Fluids Eng.*, **127**, pp. 400–403.
- [2] Zaki, T. A., Wissink, J., Rodi, W., and Durbin, P. A., 2010. "Dns of transition in a compressor cascade: The influence of free-stream turbulence". *J.Fluid Mech.*, **665**, pp. 57–98.
- [3] Zaki, T. A., Wissink, J., Durbin, P. A., and Rodi, W., 2009. "Direct computations of boundary layers distorted by migrating wakes in a linear compressor cascade". *Flow, Turbulence and Combustion*, **83**(3), pp. 307–322.
- [4] Emmons, H. W., 1951. "The laminar-turbulent transition in a boundary layer". *J.Aero.Sci.*, **18**, pp. 490–498.
- [5] Schlichting, H., 1979. *Boundary Layer Theory*. Mc-Graw Hill, New York.
- [6] Jacobs, R. G., and Durbin, P. A., 2001. "Simulations of bypass transition". *J. Fluid Mech.*, **428**, pp. 185–212.
- [7] Zaki, T. A., and Saha, S., 2009. "On shear sheltering and the structure of vortical modes in single and two-fluid boundary layers". *J.Fluid Mech.*, **626**, pp. 111–147.
- [8] Zaki, T. A., and Durbin, P. A., 2005. "Mode interaction and the bypass route to transition". *J.Fluid Mech.*, **531**, pp. 85–111.
- [9] Schubauer, G. B., and Klebanoff, P. S., 1955. Contributions on the mechanics of boundary layer transition. Tech. Note TN 3489, NACA.
- [10] Gad-elhak, M., Blackwelder, R. F., and Riley, J. J., 1981. "On the growth of turbulent regions in laminar boundary-layers". *J.Fluid Mech.*, **110**, pp. 73–95.
- [11] Sankaran, R., Sokolov, M., and Antonia, R. A., 1988. "Substructures in a turbulent spot". *J. Fluid Mech.*, **197**, pp. 389–414.
- [12] Singer, B. A., 1996. "Characteristics of a young turbulent spot". *Phys. Fluids*, **8**(2), Feb, pp. 509–521.
- [13] Ching, C. Y., and LaGraff, J. E., 1995. "Measurement of turbulent spot convection rates in a transitional boundary layer". *Exp. Thermal and Fluid Science*, **11**, pp. 52–60.
- [14] Jocksch, A., and Kleiser, L., 2008. "Growth of turbulent spots in high-speed boundary layers on a flat plate". *IJHFF*, pp. 1542–1557.
- [15] Green, M. A., Rowley, C. W., and Haller, G., 2007. "Detection of Lagrangian coherent structures in 3D turbulence". *J. Fluid Mech.*, **572**, pp. 111–120.
- [16] Volino, R. J., Schultz, M. P., and Pratt, C. M., 2003. "Conditional sampling in a transitional boundary layer under high free-stream turbulence conditions". *ASME J.Fluids Eng.*, **125**, pp. 405–416.
- [17] Rehill, B., Walsh, E. J., Nolan, K., McEligot, D. M., Brandt, L., Schlatter, P., and Henningson, D. S., 2009. "Entropy generation rate in turbulent spots in a boundary layer subject to freestream turbulence". In Proceedings of the Seventh IUTAM Symposium on Laminar-Turbulent Transition, Vol. 18, Springer, pp. 557–560.
- [18] Gutmark, E., and Blackwelder, R. F., 1987. "On the structure of a turbulent spot in a heated laminar boundary layer". *Exp.Fluids*, **5**, pp. 217–222.
- [19] Levin, O., and Henningson, D. S., 2007. "Turbulent spots in the asymptotic suction boundary layer". *J. Fluid Mech.*, **584**, pp. 397–413.
- [20] Brandt, L., Schlatter, P., and Henningson, D. S., 2004. "Transition in boundary layers subject to freestream turbulence". *J.Fluid Mec.*, **517**, pp. 167–198.
- [21] Hernon, D., and Walsh, E. J., 2007. "Enhanced energy dissipation rates in laminar boundary layers subjected to elevated levels of freestream turbulence". *Fluid Dynamics Research*, **39**(4), p. 305.
- [22] Nolan, K. P., Walsh, E. J., and McEligot, D. M., 2010. "Quadrant analysis of a transitional boundary layer subject to free-stream turbulence". *J.Fluid Mech.*, **658**, pp. 310–335.
- [23] Hunt, J. C. R., Wray, A. A., and Moin, P., 1988. "Eddies, stream, and convergence zones in turbulent flows". *Center for Turbulence Research Rep. CTR-S88*.
- [24] Jeong, J., and Hussein, F., 1995. "On the identification of a vortex". *J. Fluid Mech.*, **285**, pp. 69–94.
- [25] Haller, G., 2002. "Lagrangian coherent structures from approximate velocity data". *Phys. Fluids*, **14**(6), pp. 1851–1861.
- [26] Seifert, A., Zilberman, M., and Wygnanski, I., 1994. "On the simultaneous measurements of two velocity components in the turbulent spot". *J.Engr. Math.*, **28**, pp. 43–54.
- [27] Schroder, A., and Kompenhans, J., 2004. "Investigation of a turbulent spot using multi-plane stereo particle image velocimetry". *Exp.Fluids*, **36**, pp. 82–90.
- [28] Matsubara, M., and Alfredsson, P. H., 2001. "Disturbance growth in boundary layers subjected to free-stream turbulence". *J. Fluid Mech.*, **430**, pp. 149–168.
- [29] Denton, J. D., 1993. "Loss mechanisms in turbomachines". *J. Turbomachinery*, **115**, pp. 621–657.